Electronic Journal of Biotechnology 28 (2017) 113–119

Contents lists available at ScienceDirect

Electronic Journal of Biotechnology

Research article

Molecular characterization of *CHST11* and its potential role in nacre formation in pearl oyster *Pinctada fucata martensii*

Qingheng Wang [1], Chuangye Yang [1], Ruijuan Hao, Zhe Zheng, Yu Jiao, Xiaodong Du *, Yuewen Deng, Ronglian Huang

Fishery College, Guangdong Ocean University, Zhanjiang, Guangdong 524088, China

ARTICLE INFO

Article history:
Received 12 March 2017
Accepted 6 June 2017
Available online 15 June 2017

Keywords:
Biomineral
Biomineralization
Carbohydrate sulfotransferase 11
Chondroitin sulfate
Chondroitin-4-sulfotransferase-1 (C4ST-1)
Mantle tissue
Molluscs
Proteoglycans
Real-time PCR
RNA interference

ABSTRACT

Background: C4ST-1 catalyzes the transfer of sulfate groups in the sulfonation of chondroitin during chondroitin sulfate synthesis. Chondroitin sulfate consists of numerous copies of negatively charged sulfonic acid groups that participate in the nucleation process of biomineralization. In the present study, we obtained two *CHST11* genes (*PmCHST11a* and *PmCHST11b*) which encoded the C4ST-1 and explored the functions of these genes in the synthesis of chondroitin sulfate and in the formation of the nacreous layer of shells.
Results: Both *PmCHST11a* and *PmCHST11b* had a sulfotransferase-2 domain, a signal peptide and a transmembrane domain. These properties indicated that these genes localize in the Golgi apparatus. Real-time PCR revealed that both *PmCHST11a* and *PmCHST11b* were highly expressed in the central zone of the mantle tissue. Inhibiting *PmCHST11a* and *PmCHST11b* via RNA interference significantly decreased the expression levels of these genes in the central zone of the mantle tissue and the concentration of chondroitin sulfate in extrapallial fluid. Moreover, shell nacre crystallized irregularly with a rough surface after RNA interference.
Conclusions: This study indicated that *PmCHST11a* and *PmCHST11b* are involved in the nacre formation of *Pinctada fucata martensii* through participating in the synthesis of chondroitin sulfate.

1. Introduction

Chondroitin sulfate proteoglycans are common in animal tissues. These proteoglycans are implicated in the development of human bone and joint diseases [1,2,3]. When negatively charged sulfonic acid groups are abundant, chondroitin sulfate participates in crystal nucleation and metal ion enrichment in biomineralization [4]. Chondroitin sulfate has a protective role in cartilage [5] by inhibiting cartilage arthritis [6]. Chondroitin-4-sulfate and chondroitin-6-sulfate exist in the organic matrix of nacre from the shell of *Haliotis rufescens* and the location of these proteoglycans indicates that chondroitin sulfate is associated with biomineralization in molluscs [7].

Carbohydrate sulfotransferase 11 (*CHST11*)/chondroitin-4-sulfotransferase-1 (C4ST-1) catalyzes the transfer of sulfate to the C-4 position of chondroitin sulfate disaccharides [8] during the synthesis of chondroitin-4-sulfate (C4S) and is involved in several biological processes [9,10,11,12]. Karlsson et al. [13] and Reynard et al. [14] reported that *CHST11* is associated with osteoarthritis and with chondrogenesis. The potential functions of acid glycosaminoglycan (GAGs) in nacre formation have been documented recently [15]. However, the role of *CHST11* in the synthesis of sulfate chondroitin and its influences on shell nacre formation are unknown.

The pearl oyster *Pinctada fucata martensii* is cultured in China and Japan for the production of nucleated pearls. In addition, *P. f. martensii* is the model species for the study of nacre formation [16]. We found that the organic matrix extracted from nacreous shells of *P. f. martensii* contain more acidic GAGs than those extracted from prismatic layers. Furthermore, the organic matrix extracted from the nacreous shells of *P. f. martensii* contained more acidic GAGs than that extracted from the shells of *Crassostrea gigas*. In addition, we detected acidic GAGs in the secretory cells of the central mantle zone of *P. f. martensii* and neutral GAGs in the mantle of *C. gigas* (unpublished). In this study, the full-length sequence of *CHST11* of *P. f. martensii* was obtained via the rapid amplification of cDNA ends (RACE) technique. We then elucidated the functions of *CHST11* in the formation of chondroitin sulfate.

* Corresponding author.
E-mail address: pearldxd@163.com (X. Du).
[1] These authors contributed equally to this work.
Peer review under responsibility of Pontificia Universidad Católica de Valparaíso.

http://dx.doi.org/10.1016/j.ejbt.2017.06.002

2. Materials and methods

2.1. Experimental animals

Adult pearl oysters were obtained from commercial farm (20°250 N, 109°570E) Dajing Xuwen, Zhanjiang, Guangdong Province, China. The animals were cultured at 25–27°C in tanks with recirculating seawater for 2–3 days before the experiment.

2.2. RNA extraction and cDNA synthesis

The animals were sacrificed for tissue sampling. The tissue samples included the marginal zone (ME) and central zone (MC) of the mantle, adductor muscle (A), gill (GI), gonad (GO) and haemocytes (B). The tissues were immediately stored in liquid nitrogen until use.

Total RNA was extracted with TRIzol reagent (Invitrogen, Carlsbad, CA, USA) in accordance with the manufacturer's instructions. RNA quantity was evaluated by measuring OD260/OD280 with a NanoDrop ND1000 spectrophotometer (ThermoFisher Scientific Inc., Waltham, MA, USA). RNA integrity was determined by fractionation on 1.0% agarose gel.

2.3. Rapid amplification of cDNA ends (RACE)

In this study, the two *CHST11* genes of pearl oyster *P. f. martensii* were designated as *PmCHST11a* and *PmCHST11b*. Primers were designed based on a partial sequence of the *CHST11* gene from the pearl sac transcriptome of *P. f. martensii* [17] and are listed in Table 1. Nested PCR was performed to increase the specificity and sensitivity of the PCR products.

Table 1
Primer list used in this study.

Primer Name	Primer Sequence (From 5′ to 3′)	Application
PmCHST11a-5′ outer	TTGAAGTTCGTTCGCTCCGACTGAATAA	5′ RACE
PmCHST11a-5′ inner	TCGCCAGAATGTAGATCCAATCTTTTCCA	5′ RACE
PmCHST11a-3′ outer	ACCGTCTCAGCATGGACTTTAGAAACAGC	3′ RACE
PmCHST11a-3′ inner	AGGGTGATGTAAGAGACCCACTGATCGC	3′ RACE
PmCHST11b-5′ outer	AAGAAATGTATGACCAAATAAGCCT	5′ RACE
PmCHST11b-5′ inner	GTTTAGCGATTATATCATAAGGTAT	5′ RACE
PmCHST11b-3′ outer	GAGACCGCAAAGGAGATGTTCCCTCTT	3′ RACE
PmCHST11b-3′ inner	TTCAAGGTTACATCCGATCCTCTTTCCAA	3′ RACE
GAPDH-S	GCAGATGGTGCCGAGTATGT	qRT-PCR
GAPDH-A	CGTTGATTATCTTGGCGAGTG	qRT-PCR
PmCHST11a-qPCR-S	TCCAAGGCGAAAAGTCCG	qRT-PCR
PmCHST11a-qPCR-A	TGTTGAAGATTCTAGCACAGCGTA	qRT-PCR
PmCHST11b-qPCR-S	TAGATTTCCATTGGCAACCTTT	qRT-PCR
PmCHST11b-qPCR-A	CGAGTTATTTGTACGGTGTTGATG	qRT-PCR
RNAi-RFP-S	GCGTAATACGACTCACTATAGGG CTGTCCCCCCAGTTCCAGTAC	RNAi
RNAi-RFP-A	GCGTAATACGACTCACTATAGGG CGTTGTGGGAGGTGATGTCCAGCT	RNAi
RNAi-*PmCHST11a*-S	GCGTAATACGACTCACTATAGGGAAAAGTCCG TTTGATATACCACCAG	RNAi
RNAi-*PmCHST11a*-A	GCGTAATACGACTCACTATAGGGGAGCGTTGA AATAGTCATCTACCGT	RNAi
RNAi-*PmCHST11b*-S	GCGTAATACGACTCACTATAGGGCGGGTAGAC TTGTAGATTTCCATTG	RNAi
RNAi-*PmCHST11b*-A	GCGTAATACGACTCACTATAGGGGCGGCAGAA AGATAGTACAAACG	RNAi

Notes: the sequences underlined are the T7 promoter sequence.

To prepare the single-strand cDNA template for RACE reactions, total RNA was extracted from mantle tissue with SMART RACE cDNA Amplification Kit (Takara, Dalian, China) in accordance with the manufacturer's instructions. The synthesized cDNA was used as the template for the first PCR reaction. The product of the first PCR reaction was used as the template for the second PCR reaction. The PCR program was executed as follows: 95°C for 5 min, 35 cycles at 95°C for 30 s, 60°C for 30 s, 72°C for 2 min and 72°C for 10 min.

2.4. DNA sequencing and sequence analysis

Purified PCR products were subcloned into a pMD-19T vector (TAKARA, Japan), transformed into DH5α and then sequenced. The full-length cDNA of the *PmCHST11* genes were obtained with DNAMAN software. BLAST program (http://www.ncbi.nlm.nih.gov/) was used to analyze the full-length cDNA of *PmCHST11* genes. The open reading frame (ORF) was identified by using the ORF finder (http://www.ncbi.nlm.nih.gov/gorf/orfig.cgi). The amino acid sequence was characterized with DNAMAN. SMART (http://smart.embl-heidelberg.de/smart/set_mode.cgi) and the TMHMM Server v.2.0 (http://www.cbs.dtu.dk/services/TMHMM/) were used to study the domain of the detected peptide and the transmembrane domain of the *PmCHST11* genes, respectively. Multiple sequence alignments were generated with the sulfotransferase domain amino acid of each sequence by using ClustalX (http://www.ebi.ac.uk/Tools/msa/clustalo/). A phylogenetic tree was constructed using MEGA6.0 program based on the neighbor-joining method with 1000 bootstrap replicates. CHST11 from *Polymorphum gilvum* was used as the out group.

2.5. Quantitative real-time PCR (qRT-PCR) assay

The primer sequences used for the qRT-PCR assay are shown in Table 1. The qRT-PCR assay was performed on Applied Biosystems 7500/7500 Fast Real-Time System (Applied Biosystems, Foster City, CA, USA) with Thermo Scientific DyNAmo Flash SYBR Green qPCR Kit (Thermo Scientific). GAPDH was selected as the reference gene to verify the expression levels of sulfotransferase genes [18,19,20,21]. To detect gene expression patterns of *PmCHST11* genes, the comparative Ct method was used to analyze the expression levels of the genes. The Ct was defined as the PCR cycle at which the fluorescence signal crossed a threshold line that was placed in the exponential phase of the amplification curve. The Ct values for the *PmCHST11* genes and the GAPDH gene were determined for each sample. The expression of *PmCHST11* genes were calculated by the $2^{-\Delta Ct}$ method with GAPDH as the reference gene. The PCR program was conducted as follows: 5 min at 95°C and 40 cycles (each cycle was for 30 s at 95°C, 15 s at 60°C and 15 s at 72°C).

2.6. RNA interference (RNAi) experiment

Sequence-specific primers for the experiment were designed and are listed in Table 1. An experimental group and two control groups were separately designed to detect the effects of *PmCHST11* expression on nacre formation. Ten animals (5–6 cm in shell length) were used per group.

PCR products were obtained by using specific primers and were purified by using EasyPure Quick Gel Extraction Kit (Thermo Scientific). dsRNA was synthesized from PCR products by using T7 RNA polymerase (Thermo Scientific). Template DNA was digested by RNase-free DNase I (Thermo Scientific). dsRNA integrity and quantity were verified as previously described. dsRNA-*PmCHST11* were diluted to 1000 ng/μL with RNase-free water and injected into the adductor of per oyster. Another injection with the same dose was performed on day 4 after the first injection. The same volume of RNase-free water and 100 μg of dsRNA-RFP in RNase-free water were separately injected [22] into oysters in the two control groups.

Total RNA was extracted from MC on day 8 after the second injection for first-strand cDNA synthesis. The expression levels of the *PmCHST11* genes after RNAi were measured via qRT-PCR. GAPDH was used as the reference gene. Gene expression was quantified via the $2^{-\Delta Ct}$ and with Rnase-free water and dsRNA-RFP as control of RNAi. Shells were collected from the different groups, washed with Milli-Q water, air-dried and then cut into pieces (0.6 cm × 0.6 cm). The shell nacre layer was observed via scanning electron microscopy (SEM) with JSM-6300 LV microscope.

Microtitration assay was used to detect the concentration of chondroitin sulfate in extrapallial fluid from each group after RNAi. Chondroitin sulfate (Sangon Biotech, China) was selected as the standard. The concentration gradient of the standard was set at 60, 80, 100, 150 and 200 mg/mL. The absorbance was set to 490 nm. Alcian blue solution was prepared by adding 10 mg alcian blue powder to 100 mL of 15% phosphoric acid and 2% sulfuric acid solution. The solution was then diluted with 50-fold with Milli-Q water. The reaction system comprised 190 μL of colorimetric solution and 10 μL of sample. The reaction time was set to 3–5 min [23,24]. To analyze the influence of RNAi on gene expression in extrapallial fluid, the concentration of sulfate chondroitin was detected with RNase-free water and dsRNA-RFP as the RNAi controls.

2.7. Statistical analysis

One-way analysis of variance (ANOVA) was performed to determine the differences in mean *PmCHST11* gene expression among different tissues and mean *PmCHST11* gene expression among different groups after RNAi. All analyses were performed with SPSS 11.0 software. The significance level for all analyses was declared at $P < 0.05$.

3. Results

3.1. Molecular characterization and sequence analysis of PmCHST11 genes

The full length of *PmCHST11a* included a 59 bp 5′-UTR and 91 bp 3′-UTR with a 28 bp poly (A) tail. The complete *PmCHST11a* cDNA sequence contained a 1317 bp ORF that encoded 438 amino acid polypeptides (Fig. S1). *PmCHST11b* had a 1179 bp ORF that encoded 392 amino acid peptides, a 68 bp 5′-UTR and 293 bp 3′-UTR with 24 bp poly (A) (Fig. S2). The deduced amino acid sequence of both *PmCHST11a* and *PmCHST11b* contained a signal peptide, a typical sulfotransfer_2 domain (100–315, 83–285) and a transmembrane domain (7–29, 7–24).

3.2. Homologous analysis and phylogenetic tree of PmCHST11 sequences

Multiple comparisons by using the BLASTx program indicated that the deduced amino acid sequence of *PmCHST11* was homologous to that of CHST11 in the sulfotransferase family. The results of multiple sequence alignment indicated that *PmCHST11* amino acid sequences had low homology (Fig. 1). *PmCHST11a* and *PmCHST11b* shared the highest identity (51% and 32%, respectively) with CHST11 sequences from *C. gigas*. The phylogenetic tree showed that CHST11 genes in molluscs and vertebrates were separated in two branches. CHST11 genes in molluscs likely descended from a common ancestor (Fig. S3).

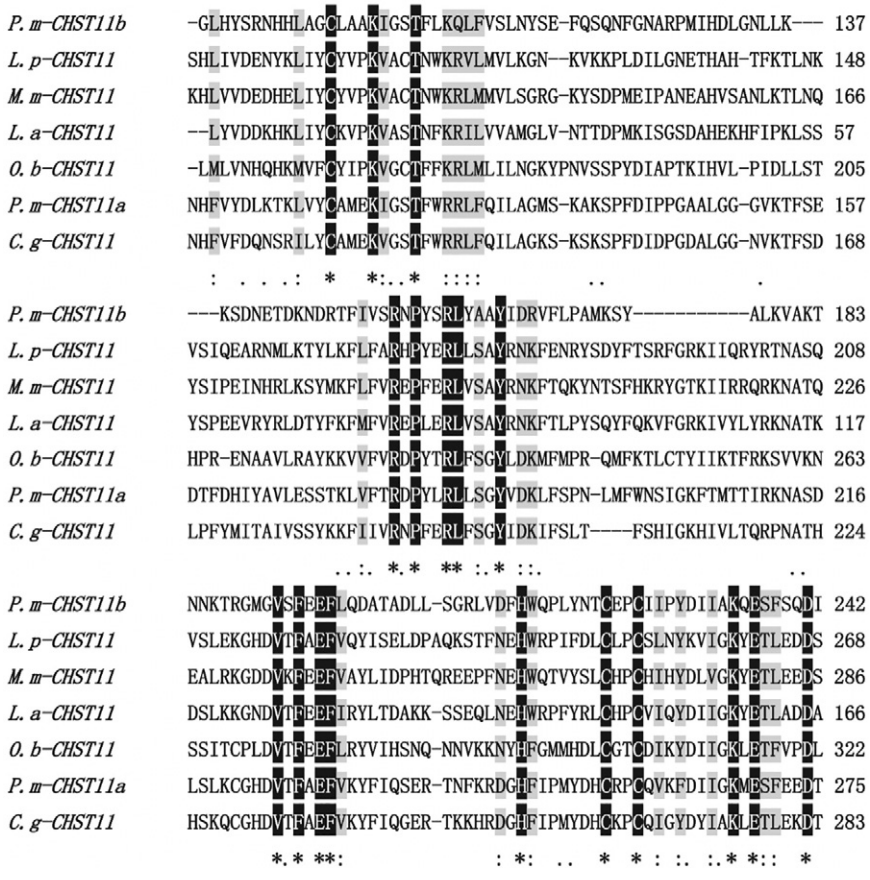

Fig. 1. Homology of the CHST11 between different species. Multiple sequence comparisons of mature CHST11 from different species (accession numbers: *Crassostrea gigas* |XP_011422059.1|, *Octopus bimaculoides*|XP_014786294.1|, *Lingula anatine*|XP_013383507.1|, *Mus musculus* |NP_067414.2| and *Limulus Polyphemus* |XP_013778038.1|). "*" and black background indicate the conserved amino acid. ":" and gray background showed amino acid with strong similarity. "." indicates amino acid with weak similarity. The numbers on the right presented the total amino acid of each protein.

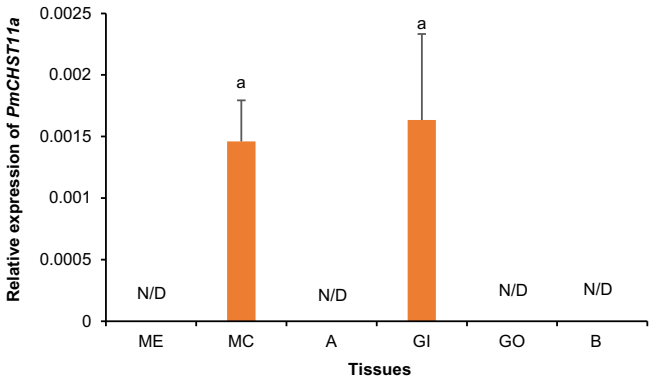

Fig. 2. Expression distribution of *PmCHST11a* at different tissues from *P. f. martensii*. ME: Marginal zone; MC: Central zone; A: Adductor muscle; GI: Gill; GO: Gonad; B: Haemocytes; Different letters indicate significantly different ($P < 0.05$) determined through one-way ANOVA and the bar represents standard deviation. Note: N/D represents that the expression of *PmCHST11a* was not detected.

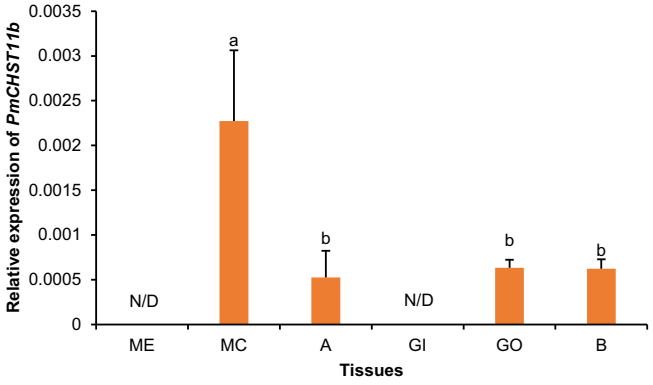

Fig. 3. Expression distribution of *PmCHST11b* at different tissues from *P. f. martensii*. ME: Marginal zone; MC: Central zone; A: Adductor muscle; GI: Gill; GO: Gonad; B: Haemocytes; Different letters indicate significantly different ($P < 0.05$) determined through one-way ANOVA and the bar represents standard deviation. Note: N/D represents that the expression of *PmCHST11b* was not detected.

3.3. Gene expression analysis of PmCHST11

qRT-PCR was performed to determine the tissue-specific expression of *PmCHST11* genes with GAPDH as the internal reference. *PmCHST11a* mRNA was expressed in the MC and GI (Fig. 2). *PmCHST11b* was highly expressed in MC compared with in other tissues ($P < 0.05$) (Fig. 3).

3.4. Relative expression of PmCHST11 genes after RNAi

To further investigate the function of *PmCHST11* genes in shell biomineralization, RNAi technology was used to inhibit the expression of *PmCHST11* genes. One control group was injected with RNase-free water, whereas the other was injected with dsRNA-RFP. qRT-PCR was used to measure the mRNA levels of *PmCHST11* genes in the MC. The expression levels of *PmCHST11* genes in the experimental group significantly decreased compared with those in the control groups (Fig. 4).

3.5. Changes in the microstructure of shell nacre after RNAi

The microstructure of shell nacre from each group was observed via SEM. The surfaces of the shells in the control groups exhibited normal, well-defined microstructure. In the nacre, small hexagonal aragonite flat tablets were densely packed together to produce a stair-like growth pattern (Fig. 5a and Fig. 5b). In the group injected with dsRNA-*PmCHST11a*, however, the shell nacre crystallized irregularly with a rough surface and exhibited C-axis growth (Fig. 5c). Disordered growth with a rough surface and changing tables was similarly observed in the shell nacre of the group injected with dsRNA-*PmCHST11b* (Fig. 5d).

3.6. Concentration of chondroitin sulfate in extrapallial fluid after RNAi

The concentrations of chondroitin sulfate in the extrapallial fluid of the three different groups are shown in Fig. 6. The concentrations of chondroitin sulfate in the dsRNA-*PmCHST11* groups were significantly lower than those in the two control groups ($P < 0.05$) (Fig. 6).

4. Discussion

C4ST-1 transfers the sulfate group from 3′-phosphoadenosine 5′-phosphosulfate to the substrate during the formation of the chondroitin sulfate proteoglycan chain. C4ST-1 participates in bone and shell formation by influencing the concentrations of chondroitin sulfate proteoglycan. In this study, we cloned the full-length sulfotransferase genes *PmCHST11a* and *PmCHST11b* from the pearl oyster *P. f. martensii*. We then explored the functions of these genes in the formation of shell nacre.

Multiple sequence alignment revealed that *PmCHST11* genes have a low homology with the *CHST11* of other species. Similar results have

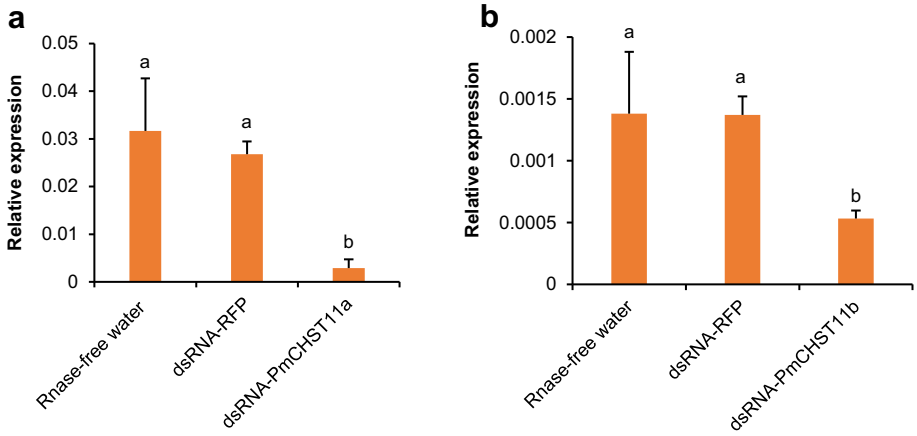

Fig. 4. The influence of RNAi on the *PmCHST11* genes relative expression. The expression of *PmCHST11a* and *PmCHST11b* in the central zone of mantle are showed in panels a and b respectively. Mean values with different letters were significantly different ($P < 0.05$).

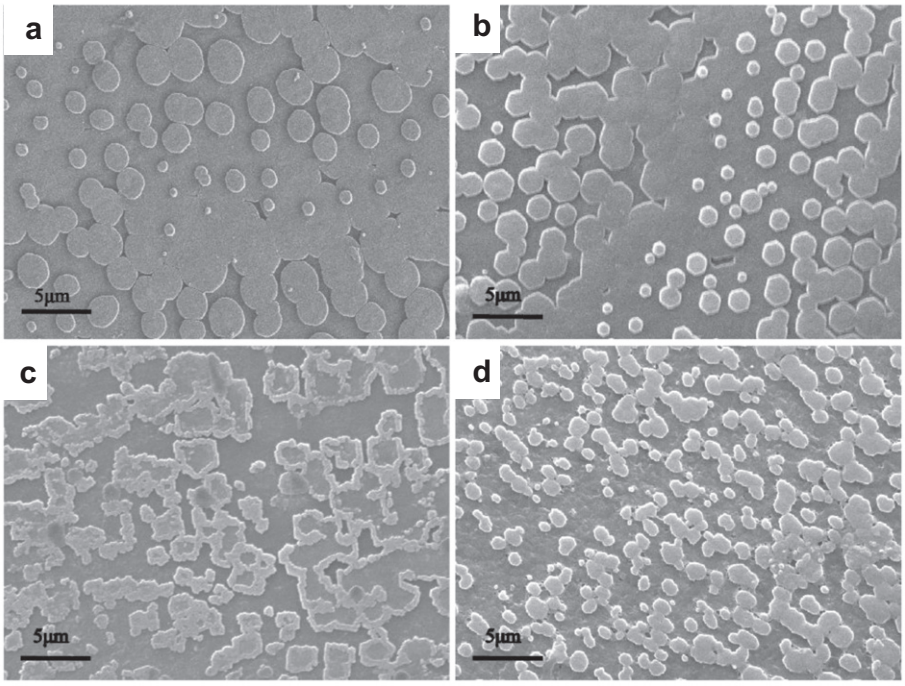

Fig. 5. The influence of RNAi on the nacre formation of the shell. Panels a and b are the microstructure of control group injected by RNase-free water and dsRNA-RFP, respectively. Panels c and d represented the microstructure of experiment group injected by dsRNA-*PmCHST11a* and dsRNA-*PmCHST11b*, respectively.

been reported in previous studies [25,26]. Furthermore, Kakuta et al. [26] found that cytosolic and membrane sulfotransferases share limited sequence similarities.

Sulfotransferases can be either cytosolic or membrane associated sulfotransferase and the membrane associated sulfotransferase in the Golgi apparatus consists of a cytosolic tail, transmembrane domain and a catalytic domain [27,28]. In this study, we found that the sequences of *PmCHST11* genes presented a typical sulfotransferase-2 domain, a signal peptide and a transmembrane domain. Therefore, *PmCHST11a* and *PmCHST11b* are membrane-associated sulfotransferases. Membrane-associated sulfotransferases sulfonate large biomolecules, such as carbohydrates and proteins [29]. For example, CHST11/C4ST1 catalyzes the transfer of sulfate groups to the 4-O position of chondroitin and dermatan sulfate [30,31,32,33]. Therefore, we propose that *PmCHST11a* and *PmCHST11b* may encode membrane-associated sulfotransferases and participate in the biosynthesis of chondroitin sulfate or sulfate dermatan.

To explore the biological functions of *PmCHST11* genes in *P. f. martensii*, we investigated the expression patterns of *PmCHST11a* and *PmCHST11b* in different tissues. GAGs are the main components of the extracellular matrix; thus, *PmCHST11b* was expressed in the adductor muscle and gonad of *P. fucata martensii*. In vertebrates, chondroitin sulfate, the product of CHST, exhibits inflammatory or anti-inflammatory immune response via the regulation of the TLR/MyD88 pathway [34,35] and adhesion with pathogens [36]. We found that *PmCHST11a* was specifically expressed in gills and that *PmCHST11b* was highly expressed in haemocytes. The gill and haemocytes are the main immune tissues of bivalves and crabs. In bivalves and crabs, the gill is direct contact with water and closely reflect environmental changes. Regnault and Durand [37] found that

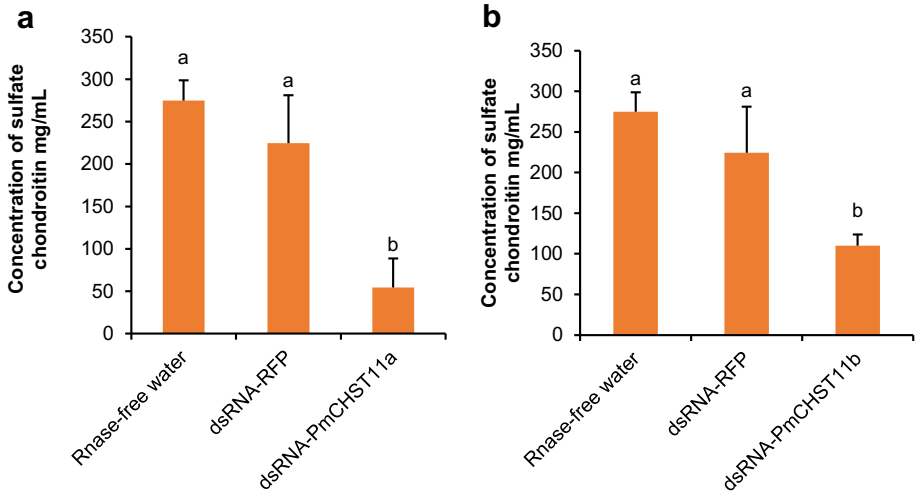

Fig. 6. The influence of RNAi on the chondroitin sulfate concentration in the extrapallial fluid. The concentration of chondroitin sulfate in the extrapallial fluid of dsRNA-*PmCHST11a* and dsRNA-*PmCHST11b* are showed panels a and b, respectively. Mean values with different letters were significantly different ($P < 0.05$).

chondroitin sulfate is a main component of GAGs in the gill and that exposure to air increases the production of chondroitin sulfate. Chondroitin sulfate has been isolated from the haemolymph of the freshwater snail [38]. Therefore, we propose that the high expression of *CHST11* genes in the gill is related to innate immunity or in pearl production.

More importantly, *PmCHST11a* and *PmCHST11b* were highly expressed in the MC, which is specifically involved in nacre formation in pearl oysters [39]. Furthermore, the majority of calcification molecules involved in nacre formation is found between the formed shell and MC. Lopes-Lima et al. [40] and Moura et al. [41] reported that glycosaminoglycan in extrapallial fluid is associated with shell formation. Sulfate anions enrich Ca^{2+} concentrations and regulate the crystal nucleation and growth of the mollusk shell [7,42]. In the present study, we found that the decrease in *PmCHST11* genes expression by RNAi caused the disordered growth of the nacreous shell layer. This result suggested that *PmCHST11* genes are closely related to nacre formation. Furthermore, the alcian blue 8GX assay revealed that the decrease in *PmCHST11* expression by RNAi consequently decreased the concentration of sulfate chondroitin glycosaminoglycan in extrapallial fluid [43]. These findings indicated that *PmCHST11* genes are involved in the synthesis of chondroitin sulfate, thus participating in nacre formation in *P. f. martensii*.

5. Conclusions

We cloned the *PmCHST11a* and *PmCHST11b* genes of the pearl oyster *P. f. martensii* for functional analysis. We found that *PmCHST11a* and *PmCHST11b* were highly expressed in the MC. After RNAi, *PmCHST11a* and *PmCHST11b* expression levels significantly decreased. Moreover, the shell nacre of the experimental group crystallized irregularly and exhibited a rough surface. Chondroitin sulfate concentration in extrapallial fluid significantly decreased in the RNAi-treated experimental group. Our results demonstrate that *PmCHST11a* and *PmCHST11b* are involved in nacre formation in *P. f. martensii*.

Conflicts of interest

The authors declare no conflict of interest.

Financial support

The study was financially supported by grants from the National Natural Science Foundation of China (31372526, 31272635 and 41206141).

Appendix A. Supplementary data

Supplementary data to this article can be found online at http://dx.doi.org/10.1016/j.ejbt.2017.06.002.

References

[1] Bauerova K, Ponist S, Kuncirova V, Mihalova D, Paulovicova E, Volpi N. Chondroitin sulfate effect on induced arthritis in rats. Osteoarthritis Cartilage 2011;19(11):1373–9. http://dx.doi.org/10.1016/j.joca.2011.08.006.
[2] Fardellone P, Zaim M, Saurel A, Maheu E. Comparative efficacy and safety study of two chondroitin sulfate preparations from different origin (avian and bovine) in symptomatic osteoarthritis of the knee. Open Rheumatol J 2013;7:1–12. http://dx.doi.org/10.2174/1874312901307010001.
[3] Lammers G, Roth G, Heck M, Zengerle R, Tjabringa GS, Versteeg EM, et al. Construction of a microstructured collagen membrane mimicking the papillary dermis architecture and guiding keratinocyte morphology and gene expression. Macromol Biosci 2012;12(5):675–91. http://dx.doi.org/10.1002/mabi.201100443.
[4] Greenfield EM, Wilson DC, Crenshaw MA. Ionotropic nucleation of calcium carbonate by Molluscan matrix. Am Zool 1984;24(4):925–32. http://dx.doi.org/10.1093/icb/24.4.925.
[5] Rovetta G, Monteforte P, Molfetta G, Balestra V. A two-year study of chondroitin sulfate in erosive osteoarthritis of the hands: Behavior of erosions, osteophytes, pain and hand dysfunction. Drugs Exp Clin Res 2004;30(1):11–6.
[6] Ronca F, Palmieri L, Panicucci P, Ronca G. Anti-inflammatory activity of chondroitin sulfate. Osteoarthritis and cartilage/OARS. Osteoarthritis Res Soc 1998;6(supp.A):14–21. http://dx.doi.org/10.1016/S1063-4584(98)80006-X.
[7] Fernandez MS, Arriagada K, Arias JL. SEM localization of proteoglycans in abalone Shell (*Haliotis rufescens*). Microsc Microanal 2007;13(S02):1462–3. http://dx.doi.org/10.1017/S1431927607071747.
[8] Klueppel M. The roles of chondroitin-4-sulfotransferase-1 in development and disease. Prog Mol Biol Transl Sci 2010;93:113–32. http://dx.doi.org/10.1016/S1877-1173(10)93006-8.
[9] Herman D, Leakey TI, Jousheghany F, Yao-Borengasser A, Cooney CA, Kieber-Emmons T, et al. DNA methylation controls CHST11 gene expression in breast cancer. Cancer Res 2012;72(8):4018. http://dx.doi.org/10.1158/1538-7445.AM2012-4018.
[10] Oliveira-Ferrer L, Hessling A, Trillsch F, Mahner S, Milde-Langosch K. Prognostic impact of chondroitin-4-sulfotransferase CHST11 in ovarian cancer. Tumor Biol 2015;36(11):9023–30. http://dx.doi.org/10.1007/s13277-015-3652-3.
[11] Zhou H, Li Y, Song X, Zhao Y, Cheng L, Zhao L, et al. CHST11/13 regulate the metastasis and chemosensitivity of human hepatocellular carcinoma cells via mitogen-activated protein kinase pathway. Dig Dis Sci 2016;61(7):1972–85. http://dx.doi.org/10.1007/s10620-016-4114-5.
[12] Tasdelen I, Berger R, Kalkhoven E. PPARγ regulates expression of carbohydrate sulfotransferase 11 (CHST11/C4ST1), a regulator of LPL cell surface binding. PLoS One 2013;8(5):e64284. http://dx.doi.org/10.1371/journal.pone.0064284.
[13] Karlsson C, Dehne T, Lindahl A, Brittberg M, Pruss A, Sittinger M, et al. Genome-wide expression profiling reveals new candidate genes associated with osteoarthritis. Osteoarthritis Cartilage 2010;18(4):581–92. http://dx.doi.org/10.1016/j.joca.2009.12.002.
[14] Reynard LN, Ratnayake M, Santibanez-Koref M, Loughlin J. Functional characterization of the osteoarthritis susceptibility mapping to CHST11—A bioinformatics and molecular study. PLoS One 2016;11(7):e159024. http://dx.doi.org/10.1371/journal.pone.0159024.
[15] Marxen JC, Hammer M, Gehrke T, Becker W. Carbohydrates of the organic shell matrix and the shell-forming tissue of the snail *Biomphalaria glabrata* (Say). Biol Bull 1998;194(2):231–40. http://dx.doi.org/10.2307/1543052.
[16] Zheng Z, Huang R, Tian R, Jiao Y, Du X. Pm-miR-133 hosting in one potential lncRNA regulates RhoA expression in pearl oyster *Pinctada martensii*. Gene 2016;591(2):484–9. http://dx.doi.org/10.1016/j.gene.2016.06.051.
[17] Zhao X, Wang Q, Jiao Y, Huang R, Deng Y, Wang H, et al. Identification of genes potentially related to biomineralization and immunity by transcriptome analysis of pearl sac in pearl oyster *Pinctada martensii*. Marine Biotechnol 2012;14(6):730–9. http://dx.doi.org/10.1007/s10126-012-9438-3.
[18] Kuchel RP, Nair S, Raftos DA. Changes in the transcriptional expression of oxidative stress response genes in Akoya pearl oysters (*Pinctada fucata*) exposed to air and mechanical agitation. Aquaculture 2012;362–363:33–8. http://dx.doi.org/10.1016/j.aquaculture.2012.07.027.
[19] Ma Z, Huang J, Sun J, Wang G, Li C, Xie L, et al. A novel extrapallial fluid protein controls the morphology of nacre lamellae in the pearl oyster, *Pinctada fucata*. J Biol Chem 2007;282:23253–63. http://dx.doi.org/10.1074/jbc.M700001200.
[20] Takeuchi T, Endo K. Biphasic and dually coordinated expression of the genes encoding major shell matrix proteins in the pearl oyster *Pinctada fucata*. Marine Biotechnol 2006;8(1):52–61. http://dx.doi.org/10.1007/s10126-005-5037-x.
[21] Anju A, Jeswin J, Thomas PC, Vijayan KK. Molecular cloning, characterization and expression analysis of F-type lectin from pearl oyster *Pinctada fucata*. Fish Shellfish Immunol 2013;35(1):170–4. http://dx.doi.org/10.1016/j.fsi.2013.03.359.
[22] Yan F, Jiao Y, Deng Y, Du X, Huang R, Wang Q, et al. Tissue inhibitor of metalloproteinase gene from pearl oyster *Pinctada martensii* participates in nacre formation. Biochem Biophys Res Commun 2014;450(1):300–5. http://dx.doi.org/10.1016/j.bbrc.2014.05.118.
[23] Gold EW. The quantitative spectrophotometric estimation of total sulfated glycosaminoglycan levels. Formation of soluble alcian blue complexes. Biochim Biophys Acta Gen Subj 1981;673:408–15. http://dx.doi.org/10.1016/0304-4165(81)90472-4.
[24] Xiong S, Jin Z. A simple spectrophotometry for determination of sulfated glycosaminoglycan concentrations. Chin J Spectrosc Lab 2005;22:1294–7.
[25] Blanchard RL, Freimuth RR, Buck J, Weinshilboum RM, Coughtrie M. A proposed nomenclature system for the cytosolic sulfotransferase (SULT) superfamily. Pharmacogenetics 2004;14(3):199–211. http://dx.doi.org/10.1097/01.fpc.0000114711.42625.c2.
[26] Kakuta Y, Pedersen LG, Pedersen LC, Negishi M. Conserved structural motifs in the sulfotransferase family. Trends Biochem Sci 1998;23(4):129–30. http://dx.doi.org/10.1016/S0968-0004(98)01182-7.
[27] Nadanaka S, Ishida M, Ikegami M, Kitagawa H. Chondroitin 4-O-sulfotransferase-1 modulates Wnt-3a signaling through control of E disaccharide expression of chondroitin sulfate. J Biol Chem 2008;283:27333–43. http://dx.doi.org/10.1074/jbc.M802997200.
[28] Paul P, Suwan J, Liu J, Dordick JS, Linhardt RJ. Recent advances in sulfotransferase enzyme activity assays. Anal Bioanal Chem 2012;403(6):1491–500. http://dx.doi.org/10.1007/s00216-012-5944-4.
[29] Chapman E, Best MD, Hanson SR, Wong CH. Sulfotransferases: Structure, mechanism, biological activity, inhibition, and synthetic utility. Angew Chem Int Ed 2004;43(27):3526–48. http://dx.doi.org/10.1002/anie.200300631.
[30] Habuchi O, Miyashita N. Separation and characterization of chondroitin 6-sulfotransferase and chondroitin 4-sulfotransferase from chick embryo cartilage. Biochim Biophys Acta Gen Subj 1982;717(3):414–21. https://doi.org/10.1016/0304-4165(82)90282-3.
[31] Hiraoka N, Nakagawa H, Ong E, Akama TO, Fukuda MN, Fukuda M. Molecular cloning and expression of two distinct human chondroitin 4-O-sulfotransferases that belong to the HNK-1 sulfotransferase gene family. J Biol Chem 2000;275:20188–96. http://dx.doi.org/10.1074/jbc.M002443200.
[32] Okuda T, Mita S, Yamauchi S, Matsubara T, Yagi F, Yamamori D, et al. Molecular cloning, expression, and chromosomal mapping of human chondroitin 4-sulfotransferase, whose expression pattern in human tissues is different

from that of chondroitin 6-sulfotransferase. J Biochem 2000;128:763–70. http://dx.doi.org/10.1093/oxfordjournals.jbchem.a022813.
[33] Yamauchi S, Mita S, Matsubara T, Fukuta M, Habuchi H, Kimata K, et al. Molecular cloning and expression of chondroitin 4-sulfotransferase. J Biol Chem 2000;275: 8975–81. http://dx.doi.org/10.1074/jbc.275.12.8975.
[34] Zhang W, Sun F, Niu H, Wang Q, Duan J. Mechanistic insights into cellular immunity of chondroitin sulfate A and its zwitterionic N-deacetylated derivatives. Carbohydr Polym 2015;123:331–8. http://dx.doi.org/10.1016/j.carbpol.2015.01.059.
[35] Vallieres M, Souich du P. Modulation of inflammation by chondroitin sulfate. Osteoarthritis Cartilage 2010;181(S1):S1–6. http://dx.doi.org/10.1016/j.joca.2010.02.017.
[36] Srinoulprasert Y, Kongtawelert P, Chaiyaroj SC. Chondroitin sulfate B and heparin mediate adhesion of *Penicillium marneffei* conidia to host extracellular matrices. Microb Pathog 2006;40(3):126–32. http://dx.doi.org/10.1016/j.micpath.2005.12.001.
[37] Regnault M, Durand F. Glycosaminoglycans in gills of an intertidal crab (*Carcinus maenas*): Changes in the GAG population in response to prolonged air exposure. J Exp Zool 1998;281(6):554–65. https://doi.org/10.1002/(SICI)1097-010X(19980815)281:6<554::AID-JEZ3>3.0.CO;2-M.
[38] Volpi N, Maccari F. Characterization of a low-sulfated chondroitin sulfate isolated from the hemolymph of the freshwater snail *Planorbarius corneus*. Mar Biol 2007; 152:1003–7. http://dx.doi.org/10.1007/s00227-007-0751-8.
[39] Barry PH, Diamond JM. A theory of ion permeation through membranes with fixed neutral sites. J Membr Biol 1971;4:295–330. http://dx.doi.org/10.1007/BF02431977.
[40] Lopes-Lima M, Ribeiro I, Pinto RA, Machado J. Isolation, purification and characterization of glycosaminoglycans in the fluids of the mollusc *Anodonta cygnea*. Comp Biochem Physiol A Mol Integr Physiol 2005;141(3):319–26. http://dx.doi.org/10.1016/j.cbpb.2005.06.007.
[41] Moura G, Vilarinho L, Santos AC, Machado J. Organic compounds in the extrapalial fluid and haemolymph of *Anodonta cygnea* (L.) with emphasis on the seasonal biomineralization process. Comp Biochem Physiol B Biochem Mol Biol 2000; 125(3):293–306. http://dx.doi.org/10.1016/S0305-0491(99)00192-3.
[42] Addadi L, Moradian J, Shay E, Maroudas NG, Weiner S. A chemical model for the cooperation of sulfates and carboxylates in calcite crystal nucleation: Relevance to biomineralization. Proc Natl Acad Sci U S A 1987;84(9):2732–6.
[43] Bjornsson S. Quantitation of proteoglycans as glycosaminoglycans in biological fluids using an alcian blue dot blot analysis. Anal Biochem 1998;256(2): 229–37. http://dx.doi.org/10.1006/abio.1997.2494.